

AD-A246 454



OFFICE OF NAVAL RESEARCH

Contract N00014-91-J-1896

R & T Code 413Q006

Technical Report No. 56

X-Ray Photoelectron Spectroscopy Study on  
The Double Layer at an  $Al_2O_3$ -Al Interface

By

Dr. David E. Ramaker

Prepared for Publication

In the

J. Vac. Sci. Technol.

George Washington University  
Department of Chemistry  
Washington, D.C.

January, 1992

Reproduction in whole or in part is permitted for  
any purpose of the United States Government

\* This document has been approved for public release  
and sale; its distribution is unlimited.

DTIC

ELECTE

FEB 24 1992

92 2 18 151

92-04212



SECURITY CLASSIFICATION OF THIS PAGE

REPORT DOCUMENTATION PAGE

1. REPORT SECURITY CLASSIFICATION Unclassified		1b. RESTRICTIVE MARKINGS	
2a. SECURITY CLASSIFICATION AUTHORITY		3. DISTRIBUTION/AVAILABILITY OF REPORT Approved for public release; distribution unlimited	
2b. DECLASSIFICATION/DOWNGRADING SCHEDULE		5. MONITORING ORGANIZATION REPORT NUMBER	
4. PERFORMING ORGANIZATION REPORT NUMBER Technical Report # 56		7a. NAME OF MONITORING ORGANIZATION Office of Naval Research (Code 418)	
6a. NAME OF PERFORMING ORGANIZATION Dept. of Chemistry George Washington Univ.		7b. ADDRESS (City, State, and ZIP Code) Chemistry Program 800 N. Quincy Street Arlington, VA 22217	
6b. ADDRESS (City, State, and ZIP Code) Washington, DC 20052		8. OFFICE SYMBOL (If applicable)	
6c. NAME OF FUNDING/SPONSORING ORGANIZATION Office of Naval Research		9. PROGRAM ELEMENT NUMBER Contract N00014-91-J-1896	
6d. ADDRESS (City, State, and ZIP Code) Chemistry Program 800 Nth, Quincy, Arlington, VA 22217		10. SOURCE OF FUNDING NUMBERS PROGRAM ELEMENT NO. TASK NO. R & T ACCESSION NO. 413Q006	
11. TITLE (Include Security Classification)		12. PERSONAL AUTHOR	
X-ray Photoelectron Spectroscopy Study on the Electrical Double Layer at an $Al_2O_3$ -Al Interface		Dr. Hideo Saabe and Dr. David E. Ramaker	
13a. TYPE OF REPORT Interim Technical		13b. TIME COVERED FROM TO	
13c. SUPPLEMENTARY NOTES Preparation for publication in J. Vac. Sci. & Technol.		14. DATE OF REPORT (Year, Month, Day) January 1992	
15. SUBJECT TERMS (Continue on reverse if necessary and identify by block number)		16. SUBJECT TERMS (Continue on reverse if necessary and identify by block number)	
17. FIELD GROUP SUB-GROUP		18. ABSTRACT (Continue on reverse if necessary and identify by block number) Upon oxidation of a clean Al surface, an electrical double layer (EDL) is formed at the $Al-Al_2O_3$ interface. This EDL is investigated using XPS data available in the literature. The EDL strength, measured as a potential difference across the EDL, depends on the Al surface and the oxidation process. The polarity of the EDL is however invariably the same: the $Al_2O_3$ side of the $Al-Al_2O_3$ interface is always positively charged. The reduction of the Al work function upon oxidation is attributed to this EDL. The asymmetry in the potential barrier shape formed in $Al-Al_2O_3$ -Al sandwiches is also attributed to a strong EDL at the electrode-film interface and a weaker EDL at the interface between the counter electrode and the film.	
20. DISTRIBUTION/AVAILABILITY OF ABSTRACT UNCLASSIFIED UNLIMITED SAME AS RPT.		21. ABSTRACT SECURITY CLASSIFICATION Unclassified	
22a. NAME OF RESPONSIBLE INDIVIDUAL Dr. Mark Ross		22b. TELEPHONE (Include Area Code) (202) 696-4409	
DD FORM 1473, 84 MAR		SECURITY CLASSIFICATION OF THIS PAGE Unclassified	

X-ray photoelectron spectroscopy study on the electrical  
double layer at an  $\text{Al}_2\text{O}_3$ -Al interface

Hideo Sambe and David E. Ramaker

Chemistry Department, George Washington University  
Washington, D. C. 20052

ABSTRACT

Upon oxidation of a clean Al surface, an electrical double layer (EDL) is formed at the Al- $\text{Al}_2\text{O}_3$  interface. This EDL is investigated using XPS data available in the literature. The EDL strength, measured as a potential difference across the EDL, depends on the Al surface and the oxidation process. The polarity of the EDL is however invariably the same: the  $\text{Al}_2\text{O}_3$  side of the Al- $\text{Al}_2\text{O}_3$  interface is always positively charged. The reduction of the Al work function upon oxidation is attributed to this EDL. The asymmetry in the potential barrier shape formed in Al- $\text{Al}_2\text{O}_3$ -Al sandwiches is also attributed to a strong EDL at the electrode-film interface and a weaker EDL at the interface between the counter electrode and the film.

Accession For	NTIS GRA&I
	DTIC TAB
	Unannounced
	Justification
By	
Distribution	
Availability	
Dist	A-1

## I. INTRODUCTION

When a pure aluminum metal is oxidized in dry  $O_2$  at room temperature, an amorphous  $Al_2O_3$  film of about 10 Å is formed on its surface [1]. At the Al- $Al_2O_3$  interface, as well as at any other phase boundaries, an electrical double layer (EDL) is expected to develop [2]. This EDL produces a potential difference (PD) across the interface and modifies the work function of Al. However, measurement of the Al work function with an oxidized Al surface generally involves not only the Al- $Al_2O_3$  interface but also the  $Al_2O_3$ -vacuum interface. In this paper, we use XPS (X-ray photoelectron spectroscopy) to investigate the PD produced across an Al- $Al_2O_3$  interface. Our XPS study, unlike the work-function measurements, can separate out the effects of the Al- $Al_2O_3$  interface from those of the  $Al_2O_3$ -vacuum interface.

The Al- $Al_2O_3$  system is chosen, simply because rather accurate XPS data are available for the aluminum-oxygen compounds [3,4]. We first present our model and later verify it with experimental results available in the literature.

## II. THEORETICAL BACKGROUND

### A. General features of XPS for oxidized Al

In XPS measurement on an oxidized Al metal, an electron-energy analyzer generally faces the oxide surface as shown in Fig. 1. The oxide ( $Al_2O_3$ ) film is generally so thin ( $\approx 10$  Å)

that electrons originating from the metal portion, as well as those from the oxide portion, can reach the analyzer.

Consequently, two peaks appear both in the Al 2p photoelectron spectrum and in the Al KLL Auger spectrum. These two peaks arise from Al atoms located in the oxide and metal portions of the sample. One can easily identify the origin (metal or oxide) of these peaks based on the expected chemical shifts for Al ( $Al^0$ ) and  $Al_2O_3$  ( $Al^{+3}$ ) and on the dependence of the relative intensity of the two peaks with change in the  $Al_2O_3$ -film thickness. Figure 2 shows two such peaks in the Al 2p photoelectron spectra. The  $Al^{+3}$  binding energies in the figure are aligned for comparison.

We denote the electron kinetic energies of the two peaks in the Al KLL Auger spectrum as  $KE(Auger, Al^0)$  and  $KE(Auger, Al^{+3})$  and those in the Al 2p photoelectron spectrum as  $KE(photo, Al^0)$  and  $KE(photo, Al^{+3})$ .  $KE(Auger)$  denotes the energy of the most intense  $KL_{23}L_{23}$  transition for an Al atom and hence does not depend on the incident X-ray energy. On the other hand,  $KE(photo)$  depends on the incident X-ray energy. However, the binding energies of the Al 2p electrons,

$$BE(Al^0) = h\nu - KE(photo, Al^0) \quad (1)$$

$$BE(Al^{+3}) = h\nu - KE(photo, Al^{+3}) \quad (2)$$

are independent of the incident X-ray energy,  $h\nu$ . In short, XPS measurements for an oxidized Al metal provide four physically significant energies:  $KE(Auger, Al^0)$ ,  $KE(Auger, Al^{+3})$ ,

$BE(Al^0)$ , and  $BE(Al^{+3})$ . We employ, however, an alternative set of four independent energies defined by

$$E(Al^0) = KE(Auger, Al^0) + BE(Al^0) \quad (3)$$

$$E(Al^{+3}) = KE(Auger, Al^{+3}) + BE(Al^{+3}) \quad (4)$$

$$E(M/O) = BE(Al^{+3}) - BE(Al^0) \quad (5)$$

$$E(O/V) = BE(Al^{+3}) \quad (6)$$

These energy parameters are more useful because, except for  $E(O/V)$ , they eliminate the static-charge referencing problem.  $E(Al^{+3})$  and  $E(Al^0)$  are nothing but the modified Auger parameters (MAP) introduced by Wagner [3] and are independent of the interfacial potentials.  $E(M/O)$  depends on only the metal-oxide interfacial potentials, as explained below.

Electrons originating from the metal portion must cross the M/O (metal-oxide) and O/V (oxide-vacuum) interfaces to reach the electron-energy analyzer (see Fig. 1), and consequently experience the potential differences (PD) across these interfaces denoted as  $PD(M/O)$  and  $PD(O/V)$ . These PDs enter in both  $KE(Auger, Al^0)$  and  $BE(Al^0)$ , since their electrons originate from the metal portion  $(Al^0)$ . However, because of Eq. (1), the PDs in  $KE(Auger, Al^0)$  and  $BE(Al^0)$  enter with opposite signs. Therefore, a sum of these energies, that is  $E(Al^0)$ , is independent of both  $PD(M/O)$  and  $PD(O/V)$ .

Electrons originating from the oxide portion  $(Al^{+3})$ , on the other hand, cross only the O/V interface on the way to the electron-energy analyzer and hence experience only  $PD(O/V)$ .

This  $PD(O/V)$  also enters in  $KE(Auger, Al^{+3})$  and  $BE(Al^{+3})$  with opposite signs, so that  $E(Al^{+3})$  is similarly independent of both  $PD(M/O)$  and  $PD(O/V)$ .

$E(M/O)$  is defined as an energy difference between  $BE(Al^{+3})$  and  $BE(Al^0)$ . Since  $PD(O/V)$  enters in  $BE(Al^{+3})$  and  $BE(Al^0)$  with the same sign, the  $PD(O/V)$  contributions cancel in  $E(M/O)$  and consequently  $E(M/O)$  does not depend on  $PD(O/V)$ . In other words,  $E(M/O)$  depends only on  $PD(M/O)$ . The  $PD(M/O)$  is expected to be stable and reproducible, while  $PD(O/V)$  is harder to obtain reproducibly because of adventitious surface contamination.

## B. Theoretical model

Let us first consider an imaginary  $Al_2O_3$ -Al system.

Suppose that a thin  $\gamma$ - $Al_2O_3$  film is made separately and then brought into contact with a clean Al surface. In this case, electron migration across the  $Al_2O_3$ -Al interface will not take place, since the Fermi level of the Al metal is situated inside the forbidden band gap of the insulator  $Al_2O_3$ , far away (more than 2 eV) from the top of the valence band (VB) and the bottom of the conduction band (CB). The electron energy diagram for this  $Al_2O_3$ -Al system is nothing but a series of energy diagrams for isolated  $\gamma$ - $Al_2O_3$  and element Al, where the vacuum level between them is eliminated, as shown in Fig. 3a. Note that, in the figure, the vacuum level (VL) connected to  $Al_2O_3$  is equal to that connected to Al. We use this imaginary  $Al_2O_3$ -Al system as a reference system.

Now, we consider a more realistic  $\text{Al}_2\text{O}_3$ -Al system: A thin  $\text{Al}_2\text{O}_3$  film is grown on a clean Al surface by exposing it to dry  $\text{O}_2$  at room temperature. It is assumed that the oxide film formed in this way is an amorphous  $\gamma$ - $\text{Al}_2\text{O}_3$  and almost homogeneous throughout except at the phase boundaries [5]. The main difference between this  $\text{Al}_2\text{O}_3$ -Al system and the reference system described above is therefore the phase boundaries. It is quite reasonable that the asymmetric forces, which are always present at phase boundaries, are adjusted in the process of the  $\text{Al}_2\text{O}_3$  film formation. Adjustment at a phase boundary normally results in the formation of EDL at the phase boundary and hence a PD across the phase boundary [2]. Consequently all of the electronic energy levels of  $\text{Al}_2\text{O}_3$  shift uniformly in comparison with those levels of  $\text{Al}_2\text{O}_3$  in the reference system (a), as shown in Fig. 3b where the uniform shift is denoted as  $\text{PD}(\text{M/O})$ . The work function of Al metal also changes by  $\text{PD}(\text{M/O}) + \text{PD}(\text{O/V})$ , where  $\text{PD}(\text{O/V})$  is due to the EDL at the O/V interface.

XPS measurements on our reference  $\text{Al}_2\text{O}_3$ -Al system would give  $E(\text{M/O})$  as  $\text{BE}(\gamma\text{-Al}_2\text{O}_3) - \text{BE}(\text{element Al})$ , where  $\text{BE}(\gamma\text{-Al}_2\text{O}_3)$  and  $\text{BE}(\text{element Al})$  are the Al 2p binding energies for the isolated  $\gamma$ - $\text{Al}_2\text{O}_3$  compound and isolated elemental Al, respectively. On the other hand, XPS measurements on the  $\text{Al}_2\text{O}_3$ -Al sample represented by Fig. 3b will yield the  $E(\text{M/O})$  energy parameter to be

$$E(\text{M/O}) = \text{BE}(\gamma\text{-Al}_2\text{O}_3) - \text{BE}(\text{element Al}) - \text{PD}(\text{M/O}). \quad (7)$$

provided that the XPS chemical states of the  $\text{Al}_2\text{O}_3$  film and the Al substrate are still those of the isolated  $\gamma$ - $\text{Al}_2\text{O}_3$  and element Al. From this equation, we obtain

$$\text{PD}(\text{M/O}) = \text{BE}(\gamma\text{-Al}_2\text{O}_3) - \text{BE}(\text{element Al}) - E(\text{M/O}). \quad (8)$$

The sign of  $\text{PD}(\text{M/O})$  is chosen to be negative when the electronic levels of  $\text{Al}_2\text{O}_3$  are lowered relative to the Fermi level of Al. The EDL at the M/O interface shown in Fig. 3b therefore gives a negative  $\text{PD}(\text{M/O})$  and the EDL at the O/V interface gives a positive  $\text{PD}(\text{O/V})$ .

The interfaces of an Al- $\text{Al}_2\text{O}_3$ -Al sandwich are closely related to those of the previous two  $\text{Al}_2\text{O}_3$ -Al systems. In a sandwich, an ultra-thin  $\text{Al}_2\text{O}_3$  film is grown on an aluminum metal (Al') by exposing its surface to  $\text{O}_2$  and then another aluminum metal (Al'') is deposited on the already grown  $\text{Al}_2\text{O}_3$  film. Therefore, the Al'- $\text{Al}_2\text{O}_3$  interface will be almost identical to the Al- $\text{Al}_2\text{O}_3$  interface represented by Fig. 3b, while the  $\text{Al}_2\text{O}_3$ -Al'' interface will be similar to the  $\text{Al}_2\text{O}_3$ -Al interface of the reference system (Fig. 3a). Figure 4a shows a simplified electron-potential-energy diagram for the Al'- $\text{Al}_2\text{O}_3$ -Al'' sandwich. In this diagram, the effect of the EDL at the  $\text{Al}_2\text{O}_3$ -Al'' interface is neglected in comparison with that at the Al'- $\text{Al}_2\text{O}_3$  interface. All electron energy levels of  $\text{Al}_2\text{O}_3$  and Al'' and also the vacuum level connected to the Al'' metal are lowered uniformly by  $\text{PD}(\text{M/O})$  due to the EDL at the Al'- $\text{Al}_2\text{O}_3$  interface. When the Al' and Al'' electrodes of the sandwich (Fig. 4a) are short-circuited, electrons flow from Al' to Al''

until the Fermi levels of these two metals coincides with each other. As a result, positive charge is left behind at the Al'-Al<sub>2</sub>O<sub>3</sub> interface and excessive electrons are built up on the Al" surface at the Al"-Al<sub>2</sub>O<sub>3</sub> interface. This pair of positive and negative charges produces a trapezoidal potential barrier between the two Al metals, as shown in Fig. 4b. Thus, the asymmetry of the potential barrier can originate from a strong double layer at the Al'-Al<sub>2</sub>O<sub>3</sub> interface. In short, there is a close connection between the potential barrier shape of the Al'-Al<sub>2</sub>O<sub>3</sub>-Al sandwich and the EDL strengths at the two phase boundaries.

### III. EXPERIMENTAL RESULTS

#### A. Modified Auger parameters $E(Al^{+3})$ and $E(Al^0)$

Wagner conducted a comprehensive survey on Auger and photoelectron energies published up to 1982 and compiled these energies and also the modified Auger parameters in Ref. [3]. The claimed accuracy of the data for aluminum-oxygen compounds is around  $\pm 0.1$  eV [4]. Table I lists the modified Auger parameters (MAP) obtained from Ref. [3,4] for Al metal and Al<sub>2</sub>O<sub>3</sub> oxides. For easier comparison, the MAP minus 1460 eV are listed.

Oxidized Al, which is denoted as Al<sub>2</sub>O<sub>3</sub>/Al in Table I, exhibits two MAPs, since it has two (metal and oxide) phases. The  $E(Al^0)$  of the oxidized Al agrees with the MAPs of pure Al

(see Table I), indicating that the metal portion of the oxidized Al was not altered significantly by oxidation as far as XPS can detect. Further, the  $E(Al^{+3})$  of oxidized Al is equal to the MAP of pure  $\gamma$ -Al<sub>2</sub>O<sub>3</sub>, which differs substantially from the MAPs of other Al<sub>2</sub>O<sub>3</sub> compounds, as seen in Table I. This confirms that an oxide film on Al is indeed a  $\gamma$ -like alumina as found previously [5]. Furthermore, this agreement also confirms that  $E(Al^{+3})$  and  $E(Al^0)$  are indeed independent of the interfacial potentials.

#### B. $E(M/O)$ and $P(M/O)$

Table II lists some of the observed  $E(M/O)$ , which is defined as the energy difference between the two Al 2p peaks (see Eq. 5). Fig. 2 exhibits these two peaks in the Al 2p spectra for the first and the last data entries in Table II. We can see clearly the difference. Also included in the figure is the Al 2p binding energy of the isolated Al metal relative to that of the isolated  $\gamma$ -Al<sub>2</sub>O<sub>3</sub> compound. The Al<sup>+3</sup> binding energies are aligned for comparison. The  $E(M/O)$  values appear to depend on the oxidation conditions. Later we will show that  $E(M/O)$  also depends on the Al surface indices (i.e., surface on which the Al<sub>2</sub>O<sub>3</sub> film grows). For the XPS measurements referenced in Table II, the Al surfaces were not well characterized. To separate out these two effects, we need more systematic measurements with well defined Al surfaces and oxidation conditions.

The  $E(M/O)$  value depends not only on  $P(M/O)$  but also on the XPS chemical states of the  $Al_2O_3$  film and the Al metal. Changes in the XPS chemical states can be monitored by measuring the MAPs. But unfortunately no such monitoring has been carried out except for the first case in Table II, which shows that the XPS chemical states of the  $Al_2O_3$  films and the Al substrate are those of pure  $\gamma-Al_2O_3$  and elemental Al as detected by XPS. Furthermore it is known that the anodic films formed on Al are also  $\gamma$ -like  $Al_2O_3$  [5]. Based on these facts, we speculate that the XPS chemical state changes of the  $Al_2O_3$  and the Al substrate contribute less than 0.5 eV to the  $E(M/O)$  value, which is the largest XPS chemical state change observed among the  $Al_2O_3$  compounds (see Table I).

The  $PD(M/O)$ 's in Table II are calculated from Eq. (8) with  $BE(\gamma-Al_2O_3)-BE(elemental Al)=0.8$  eV, which are evaluated with the data from Ref. [3]. Here we have assumed that the XPS chemical states of the  $Al_2O_3$  film and the Al substrate are the same as those of  $\gamma-Al_2O_3$  and elemental Al. The error in  $PD(M/O)$  due to this assumption could be as large as 0.5 eV as discussed in the previous paragraph. The sign of  $PD(M/O)$  is, however, invariably negative for all cases in Table II. This means that the polarity of the EDL is always the polarity shown in Fig. 3b, namely, an excess positive charge on the  $Al_2O_3$  surface and the induced counter electron charge on the Al surface.

#### C. Magnitude of $PD(O/V)$

Now, we attempt to estimate the magnitude of  $PD(O/V)$  due to an EDL at the O/V interface. The difference between  $BE(Al^{+3})$  of the  $Al_2O_3$  film and  $BE(\gamma-Al_2O_3)$  of the isolated  $\gamma-Al_2O_3$  should give  $PD(O/V)$ , provided that the following conditions are met: (a) the static-charge-referencing problem for these two measurements do not introduce errors and (b) not only the XPS chemical state but also the surface conditions of the  $Al_2O_3$  are the same as those of the isolated  $\gamma-Al_2O_3$ . Assuming that the data cited in Ref. [3] satisfy these conditions, we obtain  $PD(O/V)=+0.4$  eV. Although the error in  $PD(O/V)$  could be as large as  $\pm 0.5$  eV, we may conclude that the magnitude of  $PD(O/V)$  is substantially smaller than that of  $PD(M/O)$ .

#### D. Work function change

The work function changes ( $\Delta\phi$ ) of the three Al surfaces (111), (110), and (100) upon oxidation with a high oxygen exposure (>400 Langmuir) are about -0.2, -0.8, and -1.3 eV respectively [9,10]. In our model, the work function change ( $\Delta\phi$ ) of the oxidized Al is given by

$$\Delta\phi = PD(M/O) + PD(O/V), \quad (9)$$

as can be seen in Fig. 3b. From XPS data, we have deduced a large negative value for  $PD(M/O)$  and a small value for  $PD(O/V)$ . Therefore we expect a negative  $\Delta\phi$  for all cases agreeing with the above observations. Conversely, we may state that the work function change is mainly due to the formation of an EDL at the

Al-Al<sub>2</sub>O<sub>3</sub> interface. This statement implies that the EDL strength depends on the Al surface on which the Al<sub>2</sub>O<sub>3</sub> film grows. This is, we think, quite reasonable.

## E. Potential barrier shape for Al-Al<sub>2</sub>O<sub>3</sub>-Al sandwich

The composition of the Al-Al<sub>2</sub>O<sub>3</sub>-Al sandwich suggests a symmetric potential barrier shape. However, experiments consistently show an asymmetric potential barrier of approximately the trapezoidal barrier shape as shown in Fig. 4b [11-13]. The barrier height  $\phi_1$  at the Al'-Al<sub>2</sub>O<sub>3</sub> interface is always found to be lower than the barrier height  $\phi_2$  at the Al<sub>2</sub>O<sub>3</sub>-Al interface [11-13], as indicated in Fig. 4b. The observed value for  $\phi_2 - \phi_1$ , however, varies from 0.4 eV [11] to 1.9 eV [12] and other measurements [13] fall between these two values. In our model described in Section II.B, we have

$$\phi_2 - \phi_1 = -PD(M/O) \quad (10)$$

neglecting the effect of the weaker EDL at the Al<sub>2</sub>O<sub>3</sub>-Al interface. Since  $PD(M/O)$  was always found to be negative from the analysis of the XPS data, we expect  $\phi_2 - \phi_1 > 0$  for all cases as observed. Conversely, the main cause of the asymmetric barrier shape for Al-Al<sub>2</sub>O<sub>3</sub>-Al sandwiches can be attributed to a strong EDL formed at the Al-Al<sub>2</sub>O<sub>3</sub> interface by oxidation.

## VI. SUMMARY

XPS data, work function changes, and potential barrier shapes all consistently reveal that a strong EDL is formed at the Al-Al<sub>2</sub>O<sub>3</sub> interface upon oxidation of a clean Al surface. The EDL strength depends on the Al surface indices and the oxidation conditions. The polarity of the EDL is always found as such: a positively charged Al<sub>2</sub>O<sub>3</sub> interface surface and the counter electrons in the Al metal.

In a larger sense, this work has demonstrated for the first time that XPS can be used to investigate the interfacial potential induced between an ultra-thin film and its substrate. The photoelectron-binding-energy (or Auger-line-energy) difference of a selected atom of the film and another selected atom of the substrate directly depends on this interfacial potential. If the modified Auger parameters of the film and the substrate are unchanged, a change in the energy difference equals a change in the interfacial potential. The advantage of utilizing these (Photoelectron or Auger) energy differences is that it is independent of the surface conditions of the thin film.

## ACKNOWLEDGMENTS

This work was supported by the U. S. Office of Naval Research. The authors acknowledge Ms. Jin's assistance in preparing Fig. 2.



## REFERENCES

- [1] A. Barrie, Chem. Phys. Lett. **19**, 109 (1973).
- [2] J. O'M. Bockris and A.K.N. Reddy, Modern Electrochemistry (Plenum Press, New York, 1970) Chapt. 7.
- [3] C.D. Wagner, in Practical Surface Analysis by Auger and X-Ray Photoelectron Spectroscopy, edited by D. Briggs and V.P. Seah (John Wiley & Sons, Chichester, 1983) p. 477.
- [4] C.D. Wagner et al., J. Vac. Sci. Technol. **21**, 933 (1982).
- [5] A. Despic and V.P. Parkhutik, in Modern Aspects of Electrochemistry, No. 20, edited by J. O'M. Bockris, R.E. White and B.E. Conway (Plenum Press, New York, 1989) Chapt. 6.
- [6] G.D. Davis, W.C. Moshier, T.L. Fritz and G.O. Cote, J. Electrochem. Soc., **137**, 422 (1990).
- [7] A.C. Miller cited by B.R. Strohmeier, Appl. Surf. Sci. **40**, 249 (1989).
- [8] C. Ocal, B. Basurco and S. Ferrer, Surf. Sci. **157**, 233 (1985).
- [9] R. Michel et al., Surf. Sci. **95**, 309 (1980).
- [10] P. Hofmann, W. Wyrobisch and A.M. Bradshaw, Surf. Sci. **80**, 344 (1979).
- [11] A. Braunstein, M. Braunstein, G.S. Picus and C.A. Mead, Phys. Rev. Lett. **14**, 219 (1965); A.I. Braunstein, M. Braunstein and G.S. Picus, Phys. Rev. Lett. **15**, 956 (1965).
- [12] K.W. Shepard, J. Appl. Phys. **36**, 796 (1965).
- [13] T.E. Hartman, J. Appl. Phys. **35**, 3283 (1964).

## FIGURE CAPTIONS

FIG. 1. Configuration of sample and electron detector for typical XPS measurements on oxidized Al. The electron detector faces the oxidized surface of Al. As a result, electrons originating from the metal portion must cross the two (M/O and O/V) interfaces in order to enter the detector, while those from the oxide portion cross only the O/V interface on their way to the detector.

FIG. 2. Al 2p photoelectron spectra for air-oxidized Al and anodically oxidized Al obtained from Ref. [6]. The  $Al^0$  and  $Al^{+3}$  peaks have been attributed to electrons originating from the metal ( $Al^0$ ) and the oxide ( $Al^{+3}$ ) portions of the samples. Also included is the Al 2p binding energy of isolated Al metal relative to that of isolated  $Al_2O_3(\gamma)$ , which are taken from Ref. [3]. The  $Al^{+3}$  binding energies are aligned for comparison.

FIG. 3. Simplified electron potential energy diagrams for two distinct  $Al_2O_3$ -Al systems: For (a), the  $Al_2O_3$  film is made separately and then brought into contact with a clean Al surface; the  $Al_2O_3$  film for (b) is formed on the Al surface by exposing to  $O_2$  gas. Only in case (b) does an electrical double layer develop at the phase boundaries, especially strongly at the M/O boundary.

FIG. 4. Simplified electron potential energy diagrams for an Al-Al<sub>2</sub>O<sub>3</sub>-Al sandwich. The Al<sub>2</sub>O<sub>3</sub> film is grown on an aluminum substrate Al' by exposing to O<sub>2</sub> gas, and then another aluminum Al'' film is deposited on the already grown Al<sub>2</sub>O<sub>3</sub> film. The Al' and Al'' electrodes of the sandwich is open in (a), but short-circuited in (b).

TABLE I. The modified Auger parameters (MAP) obtained from Ref. [3] for Al metal and Al<sub>2</sub>O<sub>3</sub> compounds. For easier comparison, the MAP (in eV) minus 1460 eV are listed.

Compound	$E(\text{Al}^{+3}) - 1460\text{eV}$	$E(\text{Al}^0) - 1460\text{eV}$
Al <sub>2</sub> O <sub>3</sub> /Al	1.6	6.3a)
Al <sub>2</sub> O <sub>3</sub> /Al	1.6	6.2a)
Al <sub>2</sub> O <sub>3</sub> (γ)	1.6	---
Al <sub>2</sub> O <sub>3</sub> (α)	2.1	---
Al <sub>2</sub> O <sub>3</sub> sapphire	2.0	---
Al <sub>2</sub> O <sub>3</sub> sapphire <sup>b)</sup>	2.0	---
Al <sub>2</sub> O <sub>3</sub>	1.9	---
Al	---	6.1
Al	---	6.1
Al	---	6.2

a) Calculated from the MAP difference and the  $E(\text{Al}^{+3})$  value.

b) Heated in vacuum at 450°C.

TABLE II. Observed  $E(M/O)$  values for  $Al_2O_3$  films grown on an Al surface under various oxidation conditions.

Oxidation conditions	$E(M/O)$ [in eV]	$-PD(M/O)^a)$ [in eV]	Ref.
Air, at room temperature	2.7	1.9	[6]
$O_2$ , at room temperature	2.7	1.9	[1]
$O_2$ , at 700°C for 16 min.	3.2	2.4	[8]
$O_2$ , at 700°C for 42 min.	3.6	2.8	[8]
Anodic	3.4	2.6	[7]
Anodic, in $Na_2SO_4$	4.0	3.2	[6]

a) Calculated from Eq. (8) with  $BE(\gamma-Al_2O_3) - BE(\text{pure Al}) = 0.8$  eV obtained from Ref. [3].

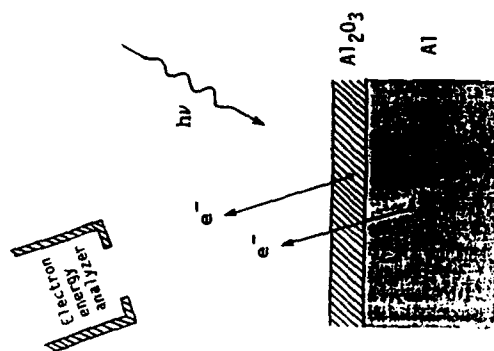


Fig. 1

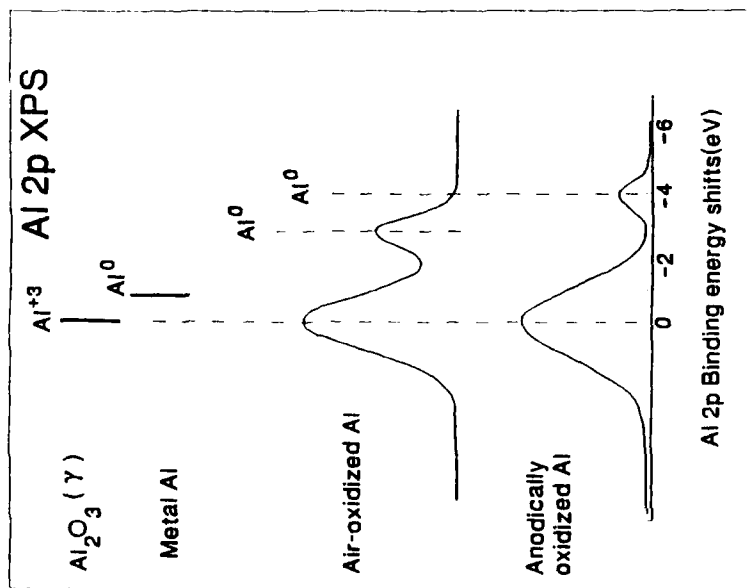


Fig. 2

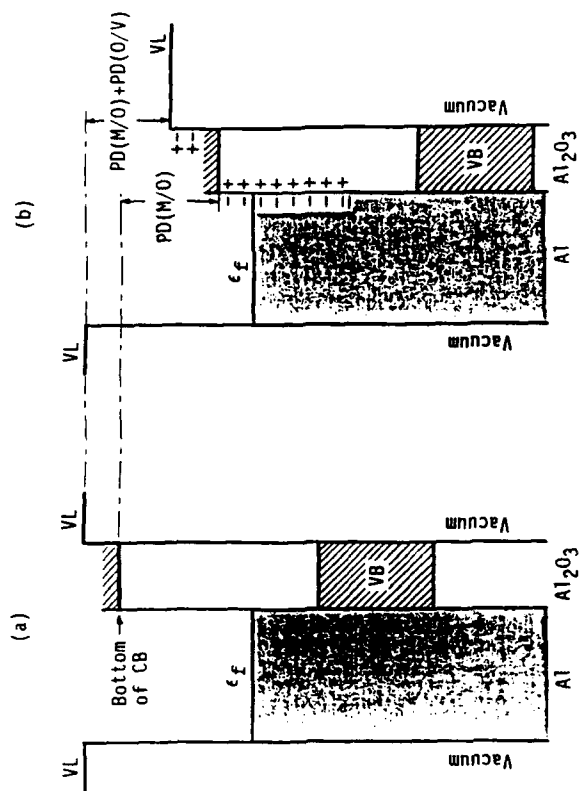


Fig. 3

# TECHNICAL REPORT DISTRIBUTION LIST - GENERAL

Office of Naval Research (2) Chemistry Division, Code 1113 800 North Quincy Street Arlington, Virginia 22217-5000	Dr. Richard W. Drisko (1) Naval Civil Engineering Laboratory Code 152 Port Hueneme, CA 93043
Dr. James S. Murday (1) Chemistry Division, Code 6100 Naval Research Laboratory Washington, D.C. 20375-5000	Dr. Harold H. Singerman (1) David Taylor Research Center Code 283 Annapolis, MD 21402-5067
Dr. Robert Green, Director (1) Chemistry Division, Code 385 Naval Weapons Center China Lake, CA 93555-6001	Chief of Naval Research (1) Special Assistant for Marine Corps Matters Code 00MC 800 North Quincy Street Arlington, VA 22217-5000
Dr. Eugene C. Fischer (1) Code 2840 David Taylor Research Center Annapolis, MD 21402-5067	Defense Technical Information Center (2) Building 5, Cameron Station Alexandria, VA 22314
Dr. Elek Lindner (1) Naval Ocean Systems Center Code 52 San Diego, CA 92152-5000	
Commanding Officer (1) Naval Weapons Support Center Dr. Bernard E. Douda Crane, Indiana 47522-5050	

\* Number of copies to forward

11

Enclosed

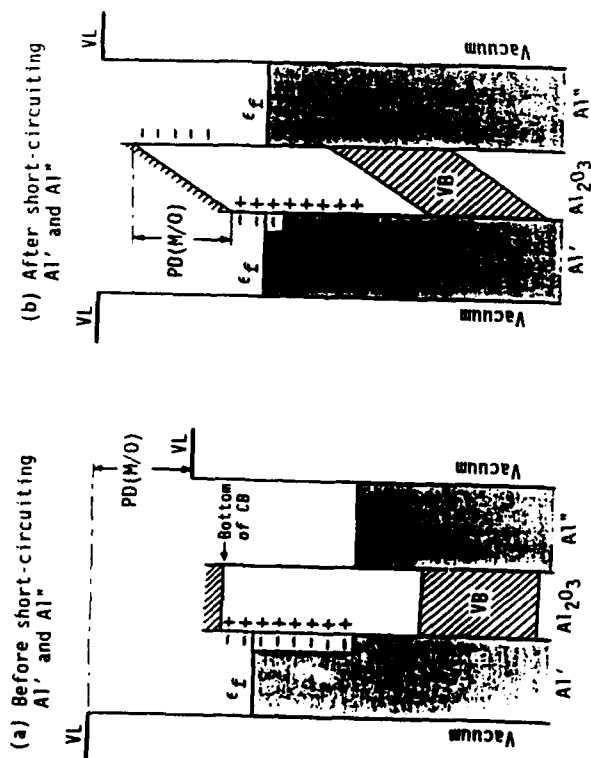


Fig. 4